3.17 A SUMMER LEAD IN THE ARCTIC OCEAN DURING THE SHEBA YEAR

Anastasia Romanou*, David M. Holland,
CAOS, Courant Inst. of Mathem. Sciences, New York University, New York
and Miles McPhee
McPhee Research Company, Naches, Washington

1. INTRODUCTION

The purpose of the present study is to simulate numerically vertical mixing below the sea-ice in a polar environment and its effect on the flux exchanges at the ocean/ice and ocean/atmosphere interfaces. Comparison is made between results from a one dimensional ocean model and observations obtained during the Surface Heat Exchange Budget of the Arctic (SHEBA) field experiment.

Vertical mixing under sea-ice is enhanced close to the ice/ocean interface and inside the oceanic mixed layer that extends between a few meters to 50-60 m. The ice-drift momentum flux and the mass flux due to formation or melting of the ice are the main stirring mechanisms for mixing there. The polar ocean mixed layer plays an important role in the global oceanic circulation and the fluxes exchanged between ice, ocean and atmosphere. Part of the mixed layer seasonal evolution involves convection and deep water formation. These processes sustain the ventilation of the deeper ocean and constitute the driving mechanism of the large scale thermohaline circulation. On the other hand, erosion of the halocline (since at cold temperatures, salinity defines the density stratification) that forms at the bottom of the mixed layer allows heat fluxes from the deeper and warmer ocean to reach the surface of the ocean and the ice that floats there. Ice melting creates such mesoscale phenomena as polynyas and reduces the albedo of the surface of the ocean allowing more shortwave radiation to be absorbed affecting the global climate.

Furthermore, even below the mixed layer, and especially in the Arctic ocean, mixing can become important. The vertical profiles of temperature show that close to the surface there is a distinguished warm water mass of (3^0C) originating from the Atlantic Ocean (Wadhams, 2002) whereas at depths 150-200 m warmer water originating from the Pacific Ocean creates such a temperature profile which potentially can lead to large thermal fluxes at the bottom pycnocline, erosion of it from below and subsequent warming of the mixed layer. It has been shown that ice growth in the Arctic is in fact limited by slow vertical mixing processes (Clayson and Kantha, 2000).

Ice plays a key role in the mixing processes; it insulates thermally the oceanic mixed layer from the atmosphere above it reducing the heat loss to the atmosphere in the winter and the heat gain during summer relative to adjacent open leads and polynyas. Ice growth and subsequent brine release at the surface of the winter mixed layer in the Arctic Ocean forces buoyancy driven convection (wintertime convection) that can reach depths of 50 m. Ice melting and freshwater flux (spring-summer mixing) to the ocean through bottom ablation and lateral melting in open leads and polynyas as well as surface snow melting result in large freshwater fluxes to the surface which tends to inhibit mixing in the mixed layer but slowly diffuses downward. Mixed layer depths are then an order of magnitude smaller than in winter. Wind forcing transfers vertically momentum to the ocean either directly (over leads polynyas) or through ice-motion that exerts surface stress to the ocean. Ice morphology with large keels (as large as 30 m (Wadhams, 2002)) provide a stirring mechanism for mixing when ice is moving through internal wave generation (Clayson and Kantha, 2000) and "slippery water" effect (McPhee and Kantha, 1989).

The first objective of the present study is to test several mixing schemes and offer suggestions for future application in ocean general circulation models (OGCMs) and coupled simulations. Large scale models become increasingly capable through increasing resolution to resolve scales of mixing in the Arctic Ocean. However the most enlighting information yet comes from process studies and field experiments such as AIDJEX,

* *Corresponding author address:* Anastasia Romanou, Center for Atmosphere-Ocean Science, Courant Inst. of Mathem. Sciences, New York University, NY 10012; e-mail:romanou@cims.nyu.edu

MIZEX, CEAREX, LEADEX and most recently SHEBA. The question addressed here is what kind of parameterizations for the vertical mixing can one use for the Arctic ocean in GCMs and coupled models to successfully model the circulation in the Arctic Ocean and be able to study feedbacks such as ice-albedo feedback on climate change.

Our goal is to use two distinct parameterizations for vertical mixing one that has been demonstrated to work in polar environments (McPhee, 1999) and the other a typical scheme used in GCMs (Canuto et al. 2002) but which has not been tested before in polar regions. To do that we are using a 1 dimensional isopycnic ocean model forced with ice and atmospheric fluxes from SHEBA to simulate a summer mixing "event" in the vicinity of a lead. Model output is then compared with SHEBA measurements of ocean heat/salt fluxes at the ice-ocean interface and at the base of the pycnocline.

In the following section a brief description is given of the SHEBA data sets that are used in the present study and the method they were obtained. The numerical model and the suggested mixing parameterizations are described in section 3. Section 4 contains the results from two idealized-forcing test cases and comparison with a different model as well as the results from the model run forced with SHEBA atmospheric and ice data from the period of July 23 - August 3, 1998 and compared to ocean SHEBA data.

2. SHEBA DATA

During SHEBA, an icebreaker was frozen into perennial ice and was left to drift with it for a full year (October 1997- October 1998). It then served as a base-research station for a research group that included atmospheric, ocean and ice investigators. The SHEBA project offered the scientific community a unique data set: a year long record of simultaneous measurements of the ice, atmospheric and oceanic one dimensional column along the SHEBA track with high temporal resolution.

Several datasets from SHEBA are used in the present study either as forcing fields or as initialization fields for the ocean model (Tabl. 1).

2.1 *Atmospheric Surface Flux Group (ASFG) tower data*

Investigators: E. Andreas, C. Fairall, O. Persson, P. Guest.

Measurements were made for the near-surface environment, regarding the wind speed and wind direction, the air temperature at 2.5 m, the latent, sensible, longwave and shortwave radiation (Persson et al., 2001). The fluxes were calculated using the observed surface pressure at one of the stations rather than an assumed constant one, the wind direction was relative to the "true" north and it accounted for the rotation of the tower during the year. Hourly averages were calculated for at least 4 10-minute periods during the hour as long as it contained two or more minutes of good data. Fluxes data were also eliminated when the airflow was from the ship or through the tower.

2.2 *Ocean current data and ice concentration from ADCP on SHEBA IOEB*

Investigators: A. Plueddmann, T. Takizawa, R. Krishfield, S. Honjo.

A 150-kHz narrow band RD Instruments Acoustic Doppler Current Profiler (ADCP) internally recorded 34,805 current ensembles in 362 days from an Ice-Ocean Environmental Buoy (IOEB) deployed during the SHEBA Experiment. The IOEB was initially deployed about 50 km from the main camp and drifted from 75.1^0 N, 141^0 W, to 80.6^0 N, 160^0 W, between October 1, 1997 and September 30, 1998. The ADCP was located at a depth of 14 m below the ice surface, and was configured to record data at 15 minute intervals from 40, 8-m wide bins, extending downward 320 m below the instrument. The retrieved raw data were processed to remove noise, correct for platform drift and geomagnetic declination, remove bottom hits, and output interpolated 2-hr average Earth-referenced current profiles along with ancillary data (Krishfield et al. 1999). Random errors in the 2 hr averaged ADCP measurements were estimated to be about 0.6 cm/s, while platform drift and Argos location uncertainty (to about 200 m) may have introduced another 1-2 cm/s of error in the absolute currents. The processing results in 4345 records at 2 hr interval at several depths between 30 m to 318 m and vertical discretization of about 8 m. The raw Argos locations were de-spiked, linearly interpolated, and smoothed with a 6 hour triangular filter.

The bathymetry data was determined from the ETOPO5 grid, while the ice concentration was obtained from the National Snow and Ice Data Center (NSIDC).

Field	Source	time interval
wind stress	Met Tower (ASFG)	hourly interpolated
zonal and meridional wind	Met Tower (ASFG)	hourly interpolated
air temperature at 10 m	Met Tower (ASFG)	hourly interpolated
longwave flux (down, up)	Met Tower (ASFG)	hourly interpolated
short wave flux (down, up)	Met Tower (ASFG)	hourly interpolated
sensible heat flux	Met Tower (ASFG)	hourly interpolated
latent heat flux	Met Tower (ASFG)	hourly interpolated
evaporation over ice	Met Tower (ASFG)	hourly interpolated
relative humidity	Met Tower (ASFG)	hourly interpolated
surface-slab skin temperature	Met Tower	hourly interpolated
ocean current data	SHEBA IOEB ADCP	2-hour interval
ice compactness	SHEBA IOEB ADCP	6-hour interval
turbulent ocean fluxes	Turbulence Mast	15-minutes interval
ice speed at ocean surface	Turbulence Mast	15-minutes interval
sea-surface temperature	CTD	10-minutes
ocean temp profiles	CTD	10-minutes
ocean saln profiles	CTD	10-minutes
cloud cover	SPO surface ship reports	6-hour interval
integrated albedo	Albedometer	once-a-day/every other day
icefloe depth or ice thickness	Ice mass balance; Pittsburgh gauge	1-2 wks (winter)/ every other day (summer)
precipitation	Nipher shielded snow gauge	once a day
ocean u,v profiles	Sonar	3-hour averages
T,S below 150 m	PHC atlas	mean monthly for SHEBA location

Table 1: Sources and description of model fluxes.

2.3 *Ocean turbulence mast data*

Investigator: M. G. McPhee

The oceanography mast experiment was designed to measure mean and turbulent quantities at multiple levels in the ocean boundary layer beneath the SHEBA ice floe, using current meters mounted along 3 mutually orthogonal axes, with nearby temperature and conductivity sensors. The clusters were mounted 4 m apart on a torsionally rigid, self-contained mast that could be lowered to arbitrary depths in the upper ocean. Each cluster sent signals to a special underwater unit to be recorded via computer. The underwater unit included compass, tiltmeters, and pressure sensor. The system sampled 6 times per second, with averaging in the deck unit reducing the data collection rate to 1 or 0.5 samples per second, depending on current velocity. More details on the system are given in McPhee (1992;1994) and McPhee and Stanton (1996).

Measurements were made from 8 Oct 97 to 28 Sep 98, with sizable gaps in February and March do to ice camp breakup and redeployment. Prior to the redeployment in late March, there were 4 clusters (from nominally 4 m to 16 m beneath the ice/ocean interface). After that, two clusters were maintained, at 4 and 8 m below the interface (but raised to 2 & 6 m during the summer). The quality of the measurements was compromised because of biofouling during the summer months and when the velocity in the boundary layer relative to the drifting ice was less than about 5 cm/s because then all three rotors were not turning consistently. The data were grouped in 15-min realizations of the turbulent flow.

2.4 *Ice Camp CTD Time Series*

Investigators: T. Stanton, D. Martinson, J. Morison, M. McPhee.

A dual sensor Sea Bird 911+ CTD was lowered automatically from the depth of the ice floe to 150 m with approximately a 10 minute cycle time. Data was collected from a microstructure package and was recorded independently on computers at Naval Postgraduate School by Jim Stockel and Jake Yazzci and at University of Washington by Roger Anderson.

The data represented 1 m vertically binned values of temperature and salinity for each downcast of the CTD

profiler. Erroneous data due to late summer biofouling were edited out.

2.5 *Ice Camp Surface Ship Weather Reports*

Investigators: R. Moritz, SHEBA Project Office, Univ. of Washington.

This data set consisted of the surface weather reports prepared at six-hour intervals by the SHEBA Project Office and coded according to the "Ship's Synoptic Code". At six hourly intervals (00, 06, 12, 18 GMT) the SHEBA Project Office weather observers aboard the Canadian Coast Guard icebreaker "Des Groseilliers" recorded the current, 10-minute average values of temperature, dew point temperature, sea level pressure, wind speed and wind direction from the SPO surface Met Tower #1 or Tower #2. The temperature and wind measurements were made at 10 meters above the surface. The observers also made visual estimates of cloud fraction, cloud base height, visibility, and current and past weather from the deck and bridge of the ship.

During the polar night, it was difficult to see clouds and other visual phenomena, so there were larger uncertainties in cloud fraction, ceiling height, cloud type, visibility and current weather in the dark periods of winter than at other times during the SHEBA year. No correction was made for the fact that there is a negative bias of approximately 5% in total cloud fraction estimated by visual observations in the Arctic winter.

2.6 *Wavelength-integrated albedo*

Investigators: D. Perovich, T. Grenfell, B. Light, J. Richter-Menge, T. Tucker.

Spectral and wavelength-integrated albedos measurements were made at least weekly every 2.5 m along a 200-m survey line from April through October, 1998. Initially this line was completely snowcovered, but as the melt season progressed it became a mixture of bare ice and melt ponds. Observed changes in albedo were the result of the seasonal transitions and the abrupt shifts resulting from synoptic weather events. Surface conditions evolved from dry snow (April-May) to melting snow (June 3) to early melt ponds (mid-late June) to fully developed melt ponds (July-August). From June through August albedo measurements were made every other day. Integrated albedos from 300 to 3000 nm were measured using a Kipp&Zonen albedometer and were accurate to within $\pm$ 0.01.

2.7 *Thickness gauges and ablation stakes*

Investigators: D. Perovich, T. Grenfell, J. Richter-Menge, T.Tucker, B. Light, H. Eicken.

This data set includes snow depth, ice surface position, ice bottom position, and pond depth measurements obtained with an ablation stake and a hot-wire thickness gauge. The ablation stake was a 3 m long wooden stake painted white with metric tape, typically installed with 1.5 m frozen in the ice and the other 1.5 m in the air. Adjacent to the ablation stake was a hot-wire thickness gauge that consisted of stainless steel wire with a steel rod attached on one end for ballast and a wooden handle on the other. The stainless steel wire was hooked to a generator that was also connected to a copper wire grounded in the ocean. The current would melt the wire free and the handle was pulled upward until the steel rod hit the bottom of the ice. The handle position was read off the ablation stake giving the position of the ice bottom. Accuracies of stake and gauge readings were typically 1 cm. Errors in measurements were due to ice blocks on the ice bottom, pressure ridges crushing the gauges and in some cases freezing of the rod into the ice. During summer several of the ablation stakes in ponds melted through the ice. The uncertainty in the measurements was $\pm$ 1-2 cm.

135 thickness gauge/ ablation stake combinations were installed and clustered at 10 sites. In the present study only data from gauges in the Pittsburgh site (the SHEBA column site with undeformed multiyear ice) are used.

2.8 *Ice Camp Daily Precipitation Amount*

Investigators: R. E. Moritz.

The daily precipitation amount (water equivalent) was measured in millimeters of liquid water equivalent using a Nipher shielded snow gauge system. The sampling rate was nominally one measurement per day. On a few occasions, the gauge was out of service (11-13 April and 18-20 August) or could not be visited for the daily observation. In these cases, the measured precipitation in the data set represented accumulation over a longer period, extending back to the time of the previous measurement. Measurements were normally made once per day, about 10:00 a.m. local time by visual inspection of the snow gauge.

The measurement site was generally about 30 m from the SHEBA Project Office 10-meter surface Met tower #1 and was moved close to it again after the ridging events of March 1998. Throughout the entire period,

the immediate environment around the snow gauge was multiyear ice of approximately 2 m thickness with typical undulating snow cover. Except during approximately 29 March - 11 April (the pressure ridge mentioned above) there were no obstructions to air flow near the gauge.

2.9 *Upper Ocean Doppler Sonar Current Observations*

Investigators: R. Pinkel, C. Halle.
Two sonar systems - a 140 Khz sonar (pre-spring 1998), and a 161 Khz sonar (after-spring 1998) were used to obtained measurements of upper ocean ice/water relative velocity. The data is given in 3 hour averages, every 2.13 m and down to 61 m depth for the first sonar and 437 m depth for the second sonar. All data that was not noise or contaminated by CTD hits is included here. The relative velocities are not true north/south velocities, but are relative to magnetic north. The North magnetic pole is assumed to be the y axis. Therefore, the current direction measured clockwise from magnetic north would be: $\theta = atan(u/v)$. The declination estimates were based on the Canadian Geomagnetic Reference Field Model, which gave
dec=$(-0.7638\ lon)+(1.1734\ (lat-75.58))+146.3895$.

2.10 *Derived datasets*

All Fluxes are taken from the SHEBA data set except T,S below 150m which are based on PHC monthly mean data and linearly interpolated to match lower SHEBA column data (Table 2).

3. MODEL DESCRIPTION

The ocean model used here is a one dimensional (vertical) isopycnic model based on the Miami Isopycnic Coordinate Model (MICOM). The vertical grid is 30 isopycnic layers of 10 m thickness each. In the traditional MICOM, all layers are isopycnic except the first layer which is the mixed layer and can obtain arbitrary density. Turbulence in the mixed layer as well as temperature, salinity and layer depth are computed via the Kraus-Turner-Gaspar scheme (Gaspar, 1988). This is a bulk parameterization scheme that assumes that the turbulence resulting from wind mixing, local shear, and buoyancy forcing is strong enough to mix uniformly all the physical properties in that layer.

3.1 *Layer thickness diffusion: the DeSzoeke shceme*

The main limitation of a bulk parameterization is that there is insufficient vertical resolution in the mixed layer (only one grid point in the vertical). To circumvent this problem, a scheme has been developed that allows for isopycnal discretization inside the mixed layer (DeSzoeke and Springer, 2002), the “purely” isopycnic layer model. A predictor-corrector method is then used for the solution of the layer thickness equation:

$$\frac{\partial}{\partial t}\Delta p = -\frac{\partial^2}{\partial \rho^2}\left(\frac{K}{\Delta p} - q\right) \tag{1}$$

whereΔp is the layer thickness, ρ is the layer density, K is the vertical diffusivity and q is the surface buoyancy forcing.

Upon discretization, where l is the layer index, the predictor and corrector values of the layer thickness are given by equations Eq. (2) and (3) respectively.

$$\Delta p_l^* = \Delta p_l^n + \frac{\Delta p_{l-1}^* - \Delta p_{l-1}^n}{2} + \frac{\Delta p_{l+1}^* - \Delta p_{l+1}^n}{2}$$

$$+\Delta t\left(-\frac{K_{l-1}}{\Delta p_{l-1}^*} + \frac{2K_l}{\Delta p_l^*} - \frac{K_{l+1}}{\Delta p_{l+1}^*}\right.$$

$$\left.-Q_{l-1} + 2Q_l - Q_{l+1}\right) \tag{2}$$

$$\Delta p_l^{n+1} = \Delta p_l^* + \frac{1}{2}(\Delta p_{l-1}^n - \Delta p_{l-1}^*)$$

$$+\frac{1}{2}(\Delta p_{l+1}^n - \Delta p_{l+1}^*) \tag{3}$$

If one substitutes for $x_l = \Delta p_l^* - \frac{2K_l\Delta t}{\Delta p_l^*}$ in Eqn. (3),

$$-x_{l-1} + 2x_l - x_{l+1} = -\Delta p_{l-1}^n + 2\Delta p_l^n - \Delta p_{l+1}^n$$

$$-2Q_{l-1}\Delta t + 4Q_l\Delta t - 2Q_{l+1}\Delta t$$

is able to obtain a solution for the intermediate layer thickness:

$$\Delta p_l^* = \frac{1}{2}[x_l + (x_l^2 + 8K_l\Delta t)^{1/2}] \tag{4}$$

total heat flux netheatflx	lw d - lw u + shw d - shw u - sbl - lathflx
net shortwave flux over ocean (W/m2)	netshw = shw d - shw u
melt rate (snow/ice freshwater flux (positive up) (m/s))	melt rate = d(ice thick)/dt * (ice cover) / 3600
ocean density	friedrich-levitus 3rd degree polynomial

Table 2: Sources and explanation of model fluxes.

The surface buoyancy flux is distributed in depth as:

$$Q_l = Q_0 q(p) + \bar{Q}$$

where $q(p) = (1 - p/p_Q, 0)$, for $p < p_Q$ where p_Q is the total depth that the surface fluxes penetrate.

3.2 *Vertical eddy viscosity and diffusivity*

The DeSzoeke scheme requires the knowledge of the rate momentum, heat and salt are diffused in the vertical direction, i.e. the vertical eddy viscosity and diffusivities. There are several turbulence closures schemes that provide K; two of which are chosen here: the Local Turbulence Scheme (LTC) by McPhee (McPhee, 1994) and the Canuto/GISS (Canuto et al., 2002) schemes.

3.2.1 *The LTC model*

The LTC model has been used extensively in polar environment studies of mixing under ice. The momentum diffusivity is K_M is the product of the friction velocity u_* and the turbulent length scale λ, where

$$u_* = \sqrt{< u'w' >} = (K_M U_z)^{1/2} \quad (5)$$

and,

$$\lambda = (1 + \frac{0.028\, u_*}{\kappa\, f\, R_c\, L})^2\, \frac{0.028\, u_*}{f} \quad (6)$$

In Eq. (5) and (6) the primed quantities are the turbulent velocities, U_z is the mean velocity shear, $L = u_*^3/(\kappa < w'b' >)$ is the Monin-Obukhov length scale and R_c = 0.2 is the critical Richardson number. The coefficients in Eq. (6) are derived based on similarity arguments and are chosen for best fit to observations in polar mixed layers (McPhee, 1992).

The relationship between the diffusivity (heat/salinity) and the viscosity is given by:

$$\frac{K_{H,S}}{K_M} = \begin{cases} 1 & : \quad R_i \leq 0.079 \\ e^{-1.5\sqrt{R_i - 0.079}} & : \quad 0.079 < R_i < 5 \\ 0.039 & : \quad R_i \geq 5 \end{cases} \quad (7)$$

where $R_i = N^2/(u_z^2 + v_z^2)$ is the Richardson number and $N^2 = -g\rho_z/\rho_0$ is the Brunt Väisälä frequency.

In the case of free convection the LTC model was extended to consider entrainment velocity $w*$ and a mixing length proportional to the mixed layer depth, if that turned out to be smaller than the one given by Eq. (6).

3.2.2 *The Canuto/GISS model*

The Canuto/GISS scheme provides an alternative calculation of the diffusivities and viscosities. It is a Reynolds stress, local closure for turbulence. Different rates for the salt and heat diffusivities are obtained based on the density ratio.

The diffusivities which are defined through the stress relations:

$$\overline{w'u'} = -KU_z\ ,\ \ \overline{w'T'} = -K_H T_z\ ,\ \ \overline{w'S'} = -K_S S_z \quad (8)$$

are only functions of the density ratio $R_\rho = \beta S_z/\alpha T_z$, the Brunt-Väisälä frequency N, the total Richardson number $Ri = N^2/(U_z^2 + V_z^2)$ and the dissipation rate ϵ.

All the turbulent fluxes are given in terms of the dissipative timescales $\tau_{(p,\theta,ps,p\theta,s\theta)}$:

- Reynolds stress, $b_{ij} = \overline{u'u'} - 2/3E\delta_{ij}$:

$$\frac{D}{Dt} b_{ij} = -\frac{8}{15} E\Sigma_{ij} - (1 - p_1)\Omega_{ij}$$

$$+(1 - p_2)Z_{ij} + \frac{1}{2} g(\alpha L_{ij} - \beta M_{ij}) - 5\tau^{-1} b_{ij}$$

- Heat flux $J_i^h = \overline{u'T'}$:

$$\frac{D}{Dt}J_i^h = -\tau_{ij}\frac{\partial T}{\partial x_j} - J_i^h U_{i,j} - (2\alpha\Psi - \beta\overline{s'T'})\frac{\partial \overline{p}}{\partial x_i} - \tau_{p\theta}^{-1}J_i^l$$

- Temperature variance $\Psi = \overline{T'^2}/2$:

$$\frac{D}{Dt}\Psi = -J_i^h\frac{\partial T}{\partial x_i} - 2\tau_\theta^{-1}\Psi$$

- Salinity variance $\Phi = \overline{s'^2}/2$:

$$J_i^s = -\tau_{ij}\frac{\partial S}{\partial x_j} - J_j^S U_{i,j} - (\alpha\overline{T's'} - 2\beta\Phi)\frac{\partial \overline{p}}{\partial x_i} - \tau_{ps}^{-1}J_i^S$$

- Salinity flux $J_i^S = \overline{u's'}$:

$$\frac{D}{Dt}J_i^s = -\tau_{ij}\frac{\partial S}{\partial x_j} - J_j^s U_{i,j} - (\alpha\overline{T's'} - 2\beta\Phi)\frac{\partial \overline{p}}{\partial x_i} - \tau_{ps}^{-1}J_i^s$$

- Temperature-Salinity correlation $\overline{T's'}$:

$$\frac{D}{Dt}\overline{T's'} = -(J_i^s\frac{\partial T}{\partial x_i} + J_i^h\frac{\partial S}{\partial x_i}) - \tau_{s\theta}^{-1}\overline{T's'}$$

  The dissipative timescales τ are computed by the integration of the respective variance spectra, e.g:

$$\tau_\theta = 2\kappa_T(\int kE_T(kdk)(\overline{T'^2})^{-1}$$

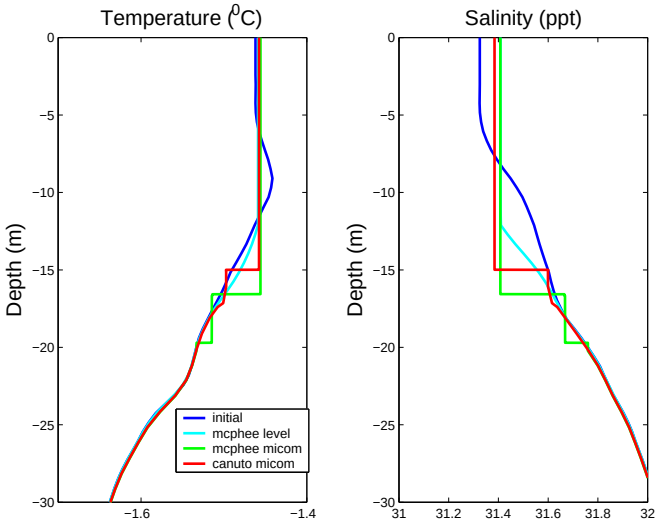

Figure 1: Test case 1: Forced convection case: (a) Temperature and (b) Salinity profiles for the test case of forced convection. The initial profile is in blue, whereas the end profiles are in green for the LTC model, red for the Canuto model and cyan for a level model using LTC.

4. RESULTS

At first two cases of idealized forcing were used to test the model performance. Then the model was forced with SHEBA data from a July event.

4.1 *Forced convection - ice motion mixing*

In this case, the ocean is assumed to be completely covered by ice, which is drifting at 10 cm/s to the east. No buoyancy flux (thermal or freshwater flux) is assumed at the surface. The initial temperature and salinity profiles correspond to SHEBA day 570 (July 23, 1998). The ocean is assumed at rest initially. The model is run for 10 days and all model results are compared to a model run of a level coordinate model using the LTC scheme.

The mixed layer deepens by about 10 m due to diffusion and erosion of the pycnocline (Fig. 1). Mixing is more energetic in the isopycnic model and the mixed layer extends to greater depths (Fig. 2). Within the isopycnic model, the McPhee scheme is more diffusive (Fig. 3). The sea surface temperature (Fig. 4) initially increases due to mixing with underlying warmer water and then decreases since the water mass below 12 m is colder. Sea surface salinity increases. All

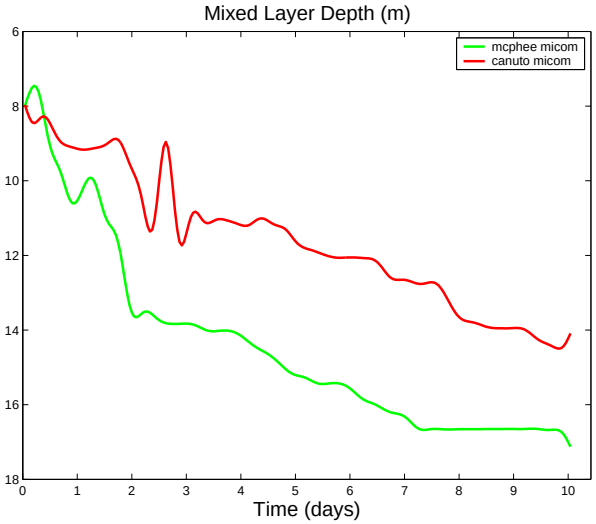

Figure 2: Test case 1: Forced convection case: Mixed layer depth evolution in the isopycnic model with the LTC parameterization (green) and the Canuto parameterization for turbulence (red).

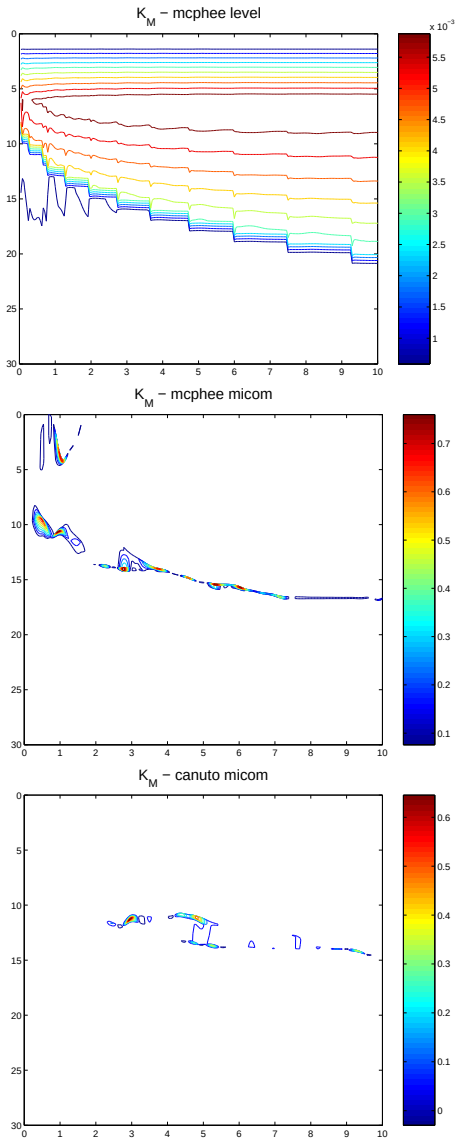

Figure 3: Test case 1: Forced convection case: Time-series of the vertical structure of the eddy diffusivities. (a) in the level model with LTC closure, (b) in the isopycnic model with LTC closure and (c) in the isopycnic model with the Canuto closure.

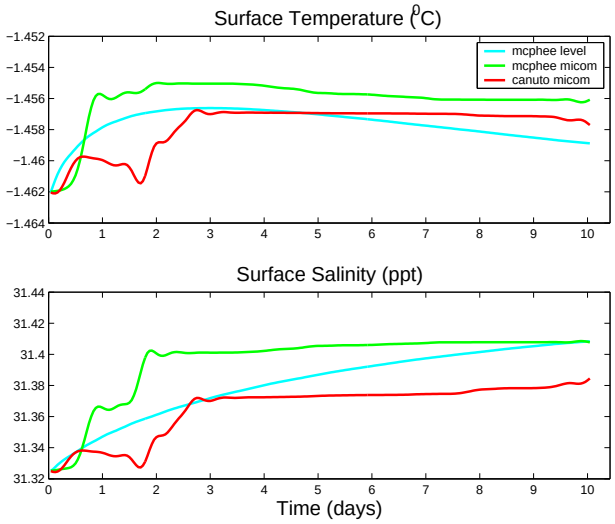

Figure 4: Test case 1: Forced convection case: (a) sea surface temperature and (b) sea surface salinity in time.

changes are more gradual in the level model and in the isopycnic model, the increase in temperature and salinity occurs faster in the LTC model.

4.2 *Free convection*

In the free convection case, the ocean is again assumed at rest initially and 100% ice covered, but the ice is motionless. Buoyancy loss is prescribed at the surface, equivalent to cooling of 200 W/m^2. Assuming that:

$$Q = \rho_0 L_f \frac{dh}{dt}$$

200 W/m^2 of cooling corresponds to ice formation and salt flux at the ice/ocean interface of 10^{-6}m/s. The initial temperature and salinity profiles correspond to SHEBA day 308 (October 30, 1997).

The salinity flux at the surface results in increasing the salinity of the mixed layer by about 1 psu; most of the increase occurs in the LTC model in both the level and the isopycnic models (Fig. 5). The mixed layer temperature does not change much in any of the three models. The pycnocline is less steep in the LTC model. The mixed layer depth however deepens irregularly (by about $\pm$ 5 m) with the Canuto scheme and only 1 m with the LTC scheme.

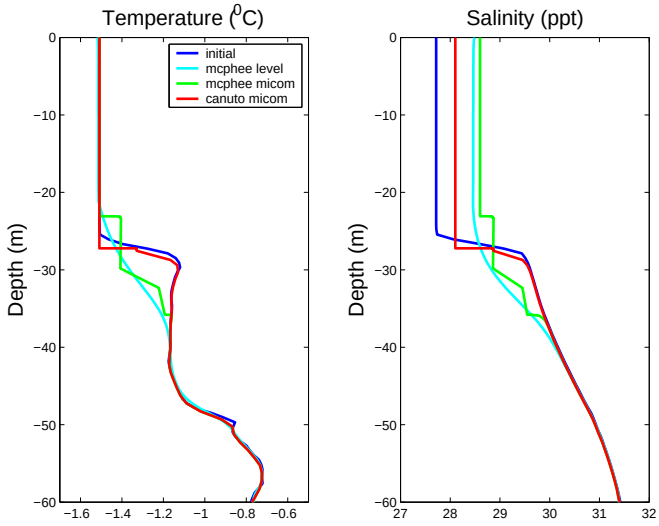

Figure 5: Test case 2: Free convection case: (a) Temperature and (b) Salinity profiles for the test case of forced convection. The initial profile is in blue, whereas the end profiles are in green for the LTC model, red for the Canuto model and cyan for a level model using LTC.

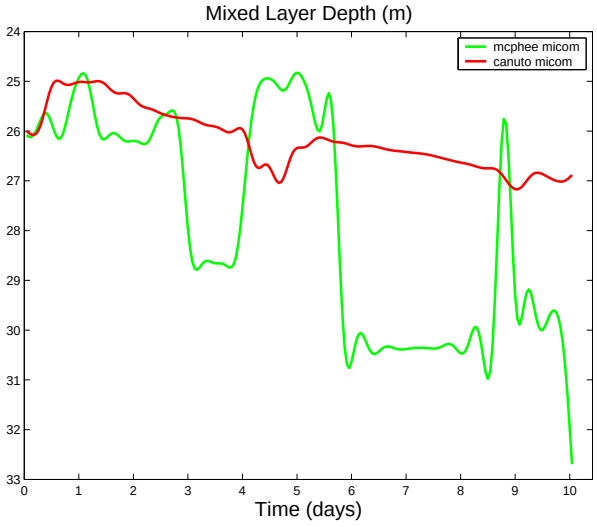

Figure 6: Test case 2: Free convection case: Mixed layer evolution with the LTC (green) and the Canuto schemes (red)

.

4.3 A SHEBA summer lead

A 10-day SHEBA period in late July - early August 1998 is chosen here to be simulated by the model. The forcing that was used to run the model during this period is shown in Figs. 7 and 8. The strong winds of about 10 m/s and large downwelling net radiation of about 200 W/m^2 despite the large cloud cover, resulted in swift ice speeds of about 0.3 m/s and ice and snow melting and significant freshwater flux into the ocean of about 1 m/s. During this time, freshwater from ice and snow melting was collected at the top of the ocean and inside open leads causing conditions of extreme stability in the upper water column. Strong wind events mixed this surface water with deeper more saline water, resulting in the freshening of the mixed layer.

The model reproduces the SHEBA salinity evolution very well (Fig. 9b and 10b). In the observations, salinity reduces gradually by about 1.5 psu over the 10 simulation period. The Canuto parameterization results in slower freshening of the mixed layer during the first 5 days and much faster than in observations during the remaining time. The model with the McPhee parameterization shows large changes in the surface salinity which follow evolution of the (prescribed) surface buoyancy flux.

With the Canuto parameterization, the mixed layer temperature is more realistic and closer to the observations, although still warmer by about 0.5^{0}C. With the LTC scheme, the mixed layer warms up by 1^{0}C (Fig. 9a and 10a).

The mixed layer depth (Fig. 11) as simulated by the Canuto mixing scheme shows abrupt changes of about 30 m over a few days corresponding to the cessation of the freshwater fluxes at the surface and the onset of stronger shear mixing due to the increased wind and ice velocities.

The mixed layer response is very sensitive to the eddy parameterization. As seen in Fig. 12, the eddy viscosities for the LTC and Canuto models are of the same order of magnitude. However, the mixed layer retreat is significantly different (Fig. 11) in the two models. Mixing in the Canuto scheme is present even during the initial freshening of the upper column. As time progresses and wind/ice mixing homogenize the upper column, the LTC model sustains turbulence much longer than the Canuto model where turbulence is intense but quickly disappears between days 572-574.

5. DISCUSSION

Two mixing schemes, the LTC (McPhee) model and the Canuto/GISS model, embedded in a “purely” isopycnic version of the MICOM model were tested in the present study under first idealized forcing and then the July 1998 SHEBA forcing.

Both mixing schemes parameterize realistically the evolution of the mixed layer properties (depth, temperature and salinity) under conditions of forced and free convection. Compared to a level model with the LTC parameterization, the

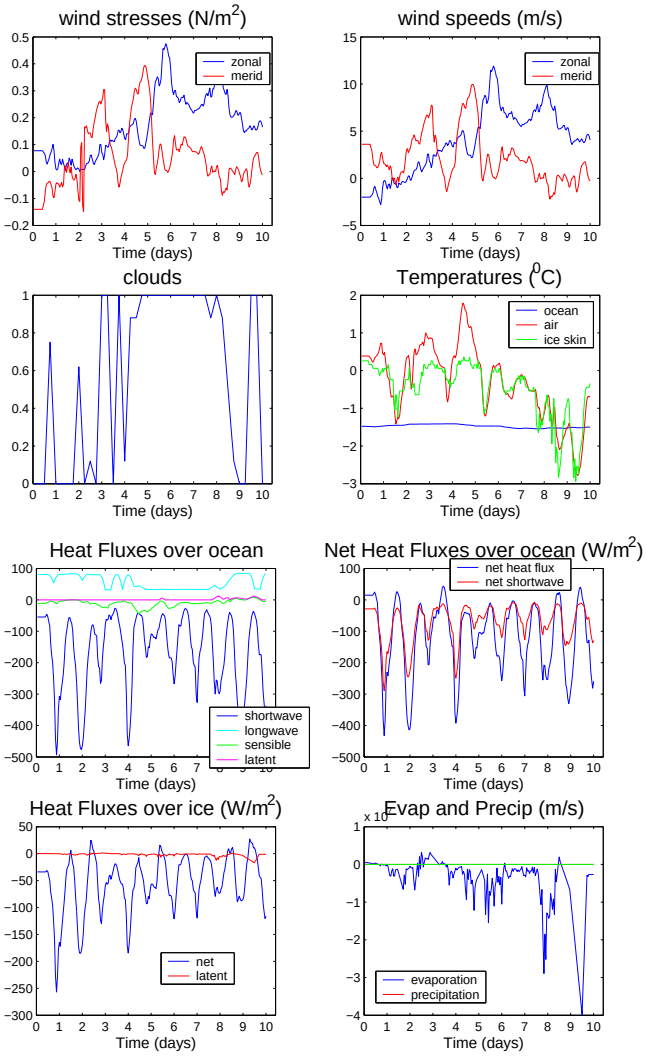

Figure 7: Atmospheric forcing during SHEBA July 23 - August 3, 1998 event.

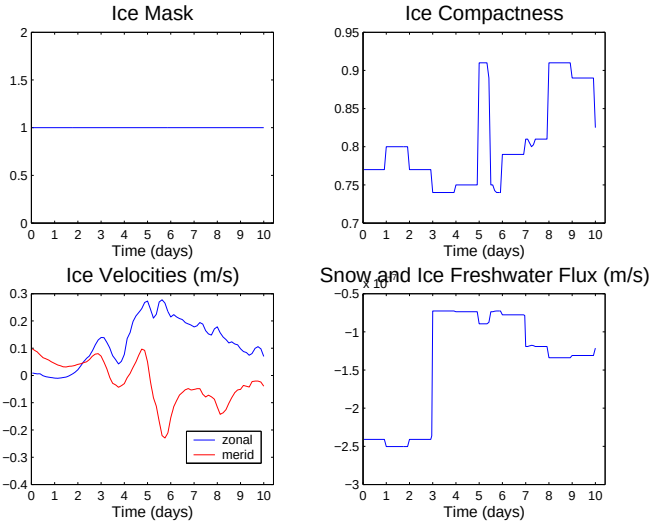

Figure 8: Ice forcing during SHEBA July 23 - August 3, 1998 event.

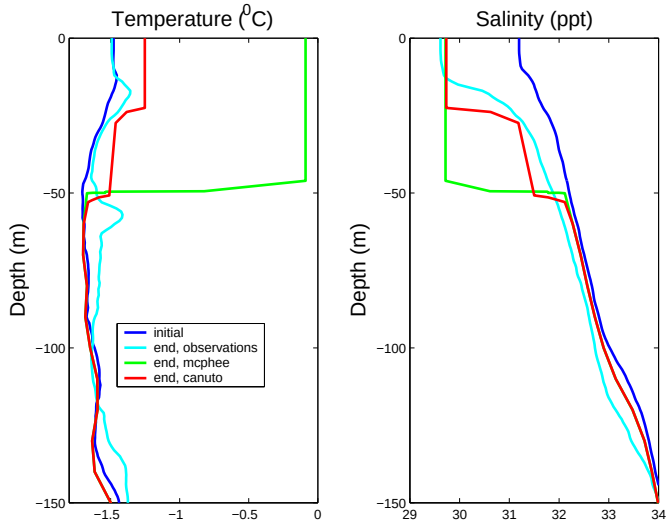

Figure 9: SHEBA case: (a) Temperature and (b) Salinity profiles at the start and the end of 10-day period in July 1998. In blue and cyan are respectively the initial and end profiles from observations. In green and red are the model final profiles with the LTC and the Canuto parameterizations respectively.

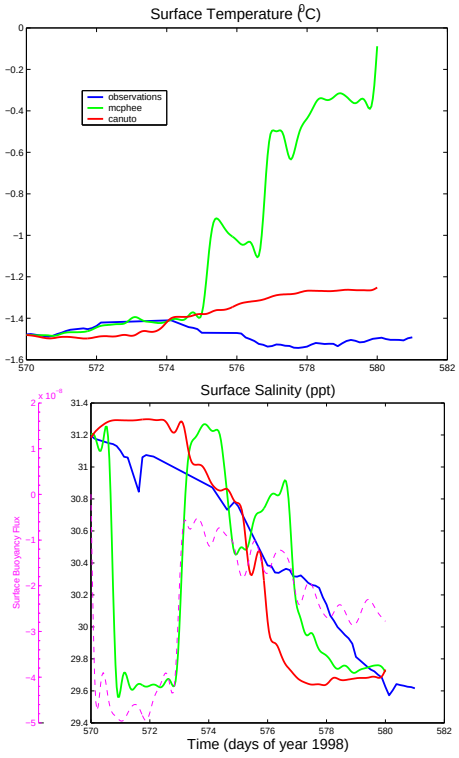

Figure 10: SHEBA case: Time series of the (a)temperature and (b)salinity evolution in the observations (blue), model with the LTC parameterization and model with the Canuto parameterization.

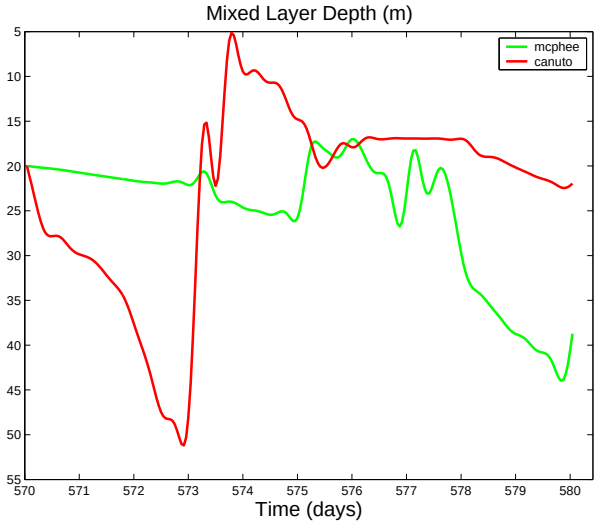

Figure 11: SHEBA case: Mixed layer depth evolution in the model with the McPhee (green) and the Canuto (red) mixing schemes

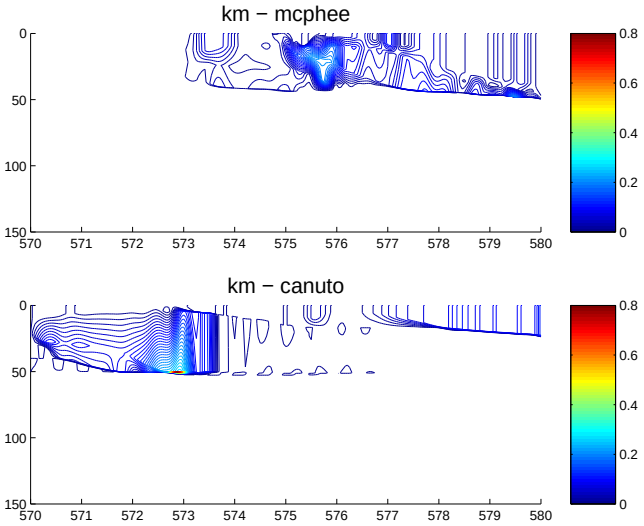

Figure 12: SHEBA case: Eddy viscosities (m^2/s) in the (a) LTC model and the (b) Canuto model.

isopycnic model was found to be more diffusive. Energetic mixing was occurring at the bottom of the pycnocline an area of important fluxes to/from the interior. Free convection was described very similarly in both the level and the isopycnic model.

The SHEBA data is an extremely valuable dataset comprised by in situ observations of the Arctic environment in a one dimensional column and during the course of a year. Little information was obtained about the three-dimensional state of the ocean during the SHEBA measurements. It is therefore challenging to simulate the ocean circulation and compare it against the SHEBA measurements because advective effects may be at some or all times important.

However, one can assume that during short periods (of a few days) with strong momentum transfer from the wind to the ocean and large freshwater convective fluxes, when the ambient ocean current is slow, these advective effects are small. One such time could be the period of July 23 - August 3, 1998, when summer melting produced large freshwater fluxes at the surface of the ocean. Strong wind mixing that occurred afterwards resulted in the freshening and warming of the ocean mixed layer significantly.

The model was proven useful in simulating SHEBA conditions from that short period of 1998. The mixed layer freshening is captured by both the LTC and the Canuto parameterizations, although the mixed layer warming is enhanced in the LTC model. The eddy viscosities in the two schemes are very similar in magnitude but the effect on the mixed layer depth and each isopycnic layer near the surface is very different.

In the light of the absence of an estimate of the advective terms during SHEBA one should be cautious in claiming the validity of one mixing scheme versus another. It is more safely said that present mixing schemes are able to simulate parts of the SHEBA mixing events and that more testing is needed.

Acknowledgements

The present work was supported by NSP grant NSF-OPP-0084286: 07/01/00-06/30/03

6. *References*

Canuto V. M., A. Howard, Y. Cheng, M. S. Dubovikov, January 2002: Ocean Turbulence. Part II: Vertical diffusivities of Momentum, Heat, Salt, Mass and Passive Scalars. Journal of Phys. Oceanog., 32, 240-264.

DeSzoeke, R. A. and S. R. Springer, 2002: A diapycnal diffusion algorithm for isopycnal ocean circulation models with special application to mixed layers. Ocean Modelling, October 2002.

Gaspar P., 1988. Modeling the Seasonal Cycle of the upper Ocean. J. Phys. Oceanog., 18, 161-180.

Kantha L. H. and C. A. Clayson, 2000: Small scale processes in Geophysical Fluid Flows; Academic Press, pp. 888.

Krishfield, R., S. Honjo, T. Takizawa, and K. Hatakeyama, IOEB Archived Data Processing and Graphical Results from April 1992 through November 1998, WHOI Tech. Rep. WHOI-99-12, 1999.

McPhee, M. G., 1999: Parameterization of mixing in the ocean boundary layer. Journal of Marine Systems, 21, 55-65.

McPhee, M.G., 1992: Turbulent Heat Flux in the Upper Ocean under Sea Ice, J. Geophys. Res., 97, 5365-5379.

McPhee, M.G., 1994: On the Turbulent Mixing Length in the Oceanic Boundary Layer, J. Phys. Oceanogr., 24, 2014-2031.

McPhee, M. G., and T. P. Stanton, 1996. Turbulence in the statically unstable oceanic boundary layer under Arctic leads, J. Geophys. Res., 101, 6409-6428.

McPhee and Kantha, 1989: Generation of internal waves by sea ice. J. Geophys. Res-Oceans, 94, C3, 3287-3302.

Persson POG, Fairall CW, Andreas EL, Guest PS, Perovich DK, 2002: Measurements near the Atmospheric Surface Flux Group tower at SHEBA: Near-surface conditions and surface energy budget, J. Geoph. Res.-Oceans, 107 (C10): art. no. 8045 SEP-OCT 2002

Uttal, T., J. A. Curry, M. G. McPhee, D. K. Perovich, R. E. Moritz, J. A. Maslanik, P. S. Guest, H. L. Stern, J. A. Moore, R. Turenne, A. Heiberg, M. C. Serreze, D. P. Wylie, O. G. Persson, C. A. Paulson, C. Halle, J. H. Morison, P. A. Wheeler, A. Makshtas, H. Welch, M. D. Shupe, J. M. Intrieri, K. Stamnes, R. W. Lindsey, R. Pinkel, W. S. Pegau, T. P. Stanton, T. C. Grenfeld, 2002: Surface heat budget of the Arctic Ocean, Bulletin of the American Meteorological Society 83 (2), 255-275.

Wadhams P., 2000: Ice in the Ocean. Taylor & Francis, pp. 364